



# Understanding space weather hazard in the Australian high-voltage power transmission lines using geomagnetic and magnetotelluric data

**Liejun Wang**

*Geoscience Australia  
Canberra  
Liejun.wang@ga.gov.au*

**Andrew Lewis**

*Geoscience Australia  
Canberra  
Andrew.Lewis@ga.gov.au*

**Bill Jones**

*Geoscience Australia  
Canberra  
Bill.Jones@ga.gov.au*

**Matthew Gard**

*Geoscience Australia  
Canberra  
Matthew.Gard@ga.gov.au*

**Jingming Duan**

*Geoscience Australia  
Canberra  
Jingming.Duan@ga.gov.au*

**Adrian Hitchman**

*Geoscience Australia  
Canberra  
Adrian.Hitchman@ga.gov.au*

## SUMMARY

Geoscience Australia's geomagnetic observatory network covers one-eighth of the Earth. The first Australian geomagnetic observatory was established in Hobart in 1840. This almost continuous 180-year period of magnetic-field monitoring provides an invaluable dataset for scientific research.

Geomagnetic storms induce electric currents in the Earth that feed into power lines through substation neutral earthing, causing instabilities and sometimes blackouts in electricity transmission systems. Power outages to business, financial and industrial centres cause major disruption and potentially billions of dollars of economic losses. The intensity of geomagnetically induced currents is closely associated with geological structure.

We modelled peak geoelectric field values induced by the 1989 Québec storm for south-eastern Australian states using a scenario analysis. Modelling shows the 3D subsurface geology had a significant impact on the magnitude of induced geoelectric fields, with more than three orders of magnitude difference across conductive basins to resistive cratonic regions in south-eastern Australia. We also estimated geomagnetically induced voltages in the Australian high-voltage power transmission lines by using the scenario analysis results. The geomagnetically induced voltages may exhibit local maxima in the transmission lines at differing times during the course of a magnetic storm depending on the line's spatial orientation and length with respect to the time-varying inducing field. Real-time forecasting of geomagnetic hazards using Geoscience Australia's geomagnetic observatory network and magnetotelluric data from the Australian Lithospheric Architecture Magnetotelluric Project (AusLAMP) helps develop national strategies and risk assessment procedures to mitigate space weather hazard.

**Key words:** Geomagnetic storms and induction hazards; Safe operation of electrical power grids

## INTRODUCTION

Geomagnetically induced currents (GICs) are the electrical currents induced in the Earth during geomagnetic storms. This phenomenon occurs with every geomagnetic storm. The impacts of extreme geomagnetic storms on critical infrastructure is of increasing concern to modern society, particularly in our present state of infrastructure development and dependence on electric power and telecommunications equipment. The most-intense and best-known modern GICs event, the 1989 "Québec storm" which occurred on 13 to 14 March 1989 during solar cycle 22, tripped circuit breakers in Hydro-Québec's electricity transmission system. The hydroelectric facility experienced a rapid loss of load which caused the voltage to suddenly increase in the hydroelectric facility and damaged transformers as result of excessive heating. The incident left the entire province of Québec without power for about nine hours (Blais and Metsa, 1993). The blackout was certainly not just a local event and power systems in the United Kingdom, United States and Sweden were also affected (Boteler, 2019).

Economic losses resulting from geomagnetic hazards are difficult to quantify. Schrijver et al. (2014) estimate that, for the US alone, in an average year "the economic impact of power-quality variations related to elevated geomagnetic activity may be several billion dollars". For a 1989 Québec-like catastrophic event, Schulte in den Bäumen et al. (2014) suggest that global economic impacts could range between US\$2.4 and \$3.4 trillion over a year. Further research is

needed to comprehensively understand and quantify such impacts across the range of susceptible sectors (Eastwood et al., 2017). However, the above figures provide an indication of the potential economic impact to modern society from GICs hazard.

The lower-to-mid latitudes occupied by the Australian continent have historically been considered low risk for extreme geomagnetic storms and consequent GICs. However, the interconnection of eastern Australian state power grids across state borders, from north Queensland to South Australia (Bartlett, 2016), has created an eastern Australia National Electricity Market (NEM) transmission system that stretches 5000 km (Figure 1). Marshall et al. (2019; 2020) have shown that such long transmission lines have increased susceptibility to GICs.

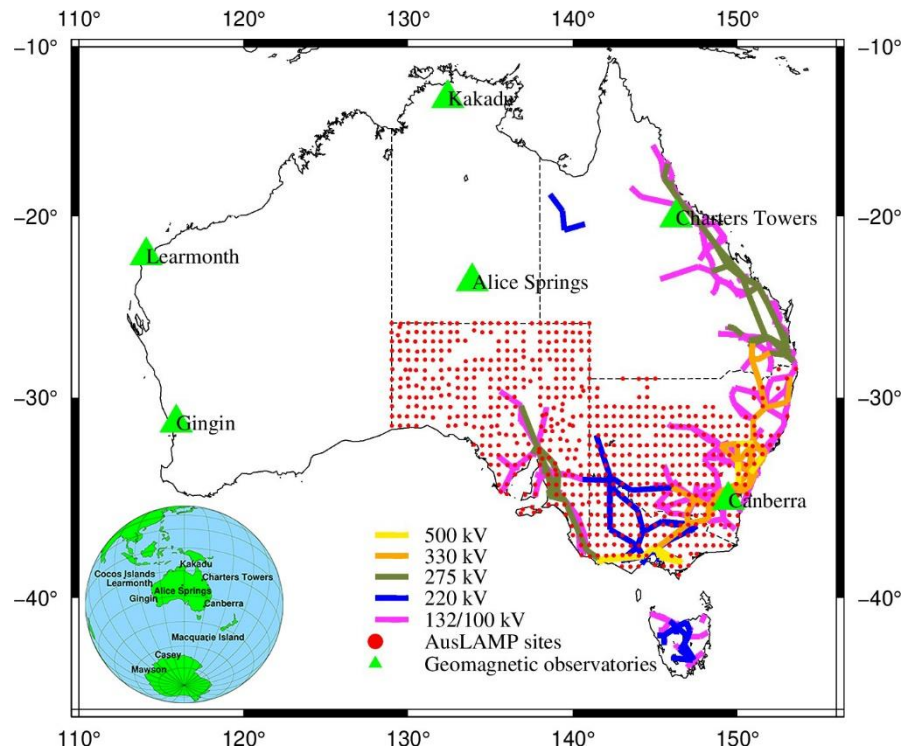


**Figure 1. Straight-line approximation networks for the Australian National Electricity Market (NEM) transmission system (Orr and Allan, 2015) used for modelling geoelectric fields. AusLAMP MT sites used in this study and the Geoscience Australia geomagnetic observatory network (insert)**

GICs depend on

- (1) the magnitude and frequency spectrum of the geomagnetic disturbance,
- (2) the Earth conductivity, and
- (3) the electrical characteristics of the power network.

Following the approach of Wang et al. (2020), this analysis focuses on the geophysical aspects of points (1) and (2) and uses a scenario analysis to estimate extreme induced geoelectric field values for South Australia, Victoria and New South Wales induced by the 1989 Québec storm. It contributes to designing and building a more resilient technological infrastructure related to the engineering aspects of point (3).

## EARTH CONDUCTIVITY

Earth conductivity, which is related to geological structure, has a great impact on GIC estimates. In general, regions with more complicated geological structure have greater hazard because of localised enhancements of the geoelectric field; for example, electrically resistive rocks near coastlines that are adjacent to deep and highly conductive oceans (Wang et al., 2016).

Figure 2 presents two depth slices (25 km and 170 km) of a broad-scale 3D model of the electrical conductivity structure of the Australian continent (Wang et al., 2014). Features include regions with more-resistive structure on Archean cratons in Western Australia and South Australia that persist to depths of around 170 km, as well as several localised high-conductivity structures at various depths. These deeper heterogeneous electrical conductivity structures and near-surface sediments, as well as the continent–ocean contrast, greatly modify the induced geoelectric fields.

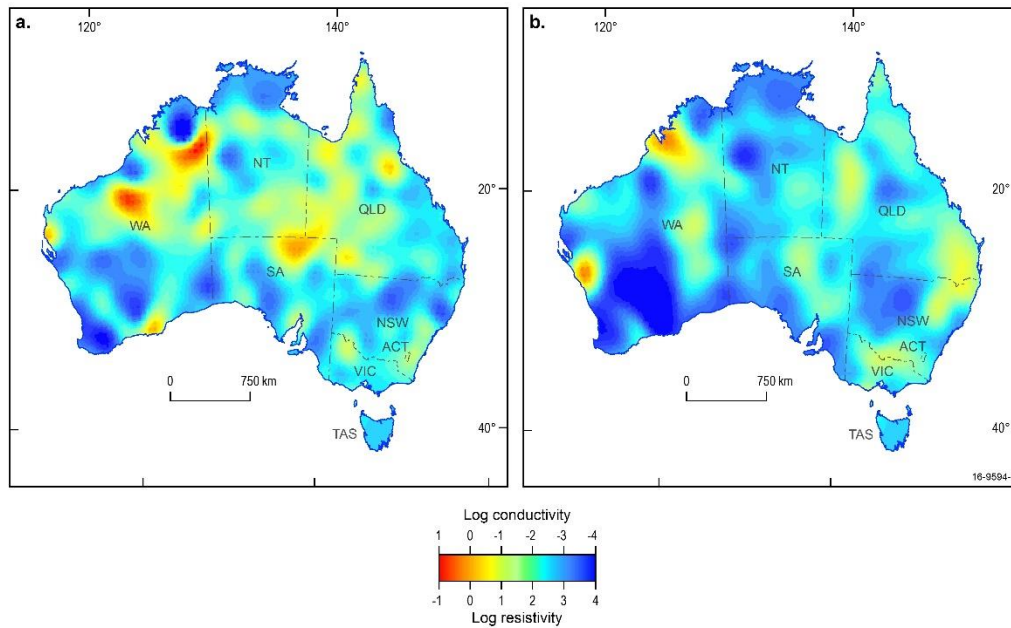


**Figure 2.** A 3D electrical conductivity model of the Australian region with conductivity images at depths of (a) 25 km and (b) 170 km. Adapted from figure 7 Wang et al. (2014).

## GEOMAGNETIC STORMS

Geomagnetic storms (or geomagnetic disturbances) result from interactions between the solar wind and electric currents in the Earth's magnetosphere and ionosphere. These interactions induce perturbations in the Earth's magnetic field that are evident at all latitudes but most pronounced at auroral and equatorial latitudes due to abnormal ionospheric conductivities in these regions (Rastogi, 2006).

Australia's geomagnetic network now comprises 10 observatories (Figure 1, insert) spanning from low latitudes (10°S) to high latitudes (67°S). The time varying geomagnetic field on the surface of the Earth consists of the main field, which originates in the Earth's core, and fields from external sources primarily generated from solar input. All these field sources are superimposed. The time varying external fields interact with geological structures at a wide range of depths and induce secondary electromagnetic fields measurable on the Earth's surface. Figure 3 presents the time varying geomagnetic field during 13 – 14 March 1989 (the 1989 Québec storm) at Canberra (CNB) and Macquarie Island (MCQ) observatories after subtracting the Earth's main field. It shows the geomagnetic disturbance at the high latitude MCQ observatory is more intense than the middle latitude CNB observatory for the same event.

## INDUCED GROUND ELECTRIC FIELDS

The magnetotelluric (MT) impedance tensor ( $Z$ ) in [mV/km]/[nT] (Cagniard, 1953) relates the surface horizontal components of the electric field ( $E$ ) in [mV/km] and the inducing magnetic field ( $B$ ) in [nT]. In this study, we use impedance tensors computed at AusLAMP sites in southern Australia to estimate the electric fields induced at these sites by magnetic fields measured during the 1989 Québec magnetic storm. We focus on magnetic-field variations in the period range 120 s to 20,000 s due to the bandwidth of the AusLAMP tensor data (Duan and Kyi, 2018; Robertson et al., 2018; Kyi et al., 2020) and the Nyquist limit of the 60 s-sampled magnetic-field data. This short-period limit is unavoidable for a scenario analysis of the 1989 Québec magnetic storm as 60 s was a common sampling rate at INTERMAGNET observatories before 1990.

For modelling GICs the important aspects of geomagnetic disturbances are their amplitude, frequency content, and spatial characteristics. We compare the intensity of ground electric fields in southern Australia using two different recordings of the same geomagnetic storm – one recorded at the CNB (mid-latitude) and the other at the MCQ (high-latitude) geomagnetic observatories, as shown in Figure 3.

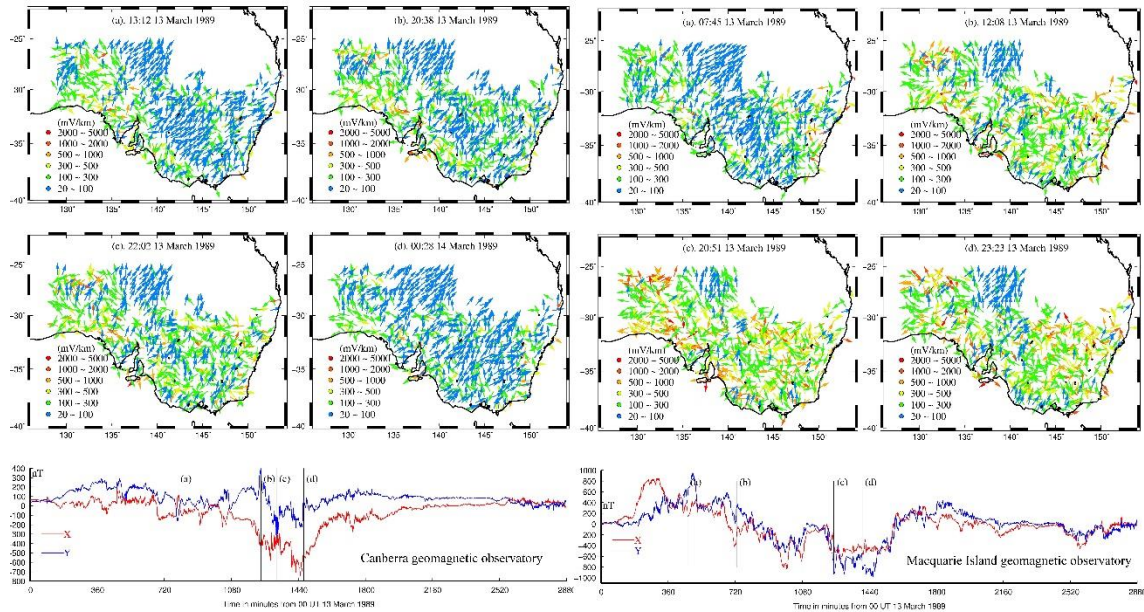


**Figure 3. Snapshots of polarisation and colour-coded amplitude of ground electric-field vectors at four selected times (a), (b), (c) and (d) induced during the 1989 Québec storm as recorded at Canberra geomagnetic observatory (left four panels) and Macquarie Island geomagnetic observatory (right four panels).**

During the course of the 1989 Québec storm, as recorded at CNB, the peak ground electric-field values computed using the AusLAMP MT tensor data are not necessarily observed simultaneously at all locations. Figure 3 shows the ground electric field computed at AusLAMP sites (left four panels). The four times selected for the figure are examples of when the peak ground electric field occurred at the majority of sites. These snapshots of the ground electric field show that the magnitude and direction of ground electric-field vectors in a sedimentary basin (blue vectors in Figure 3) are relatively consistent, and differ from other regions where 3D geological structures are dominant.

We further analyse the ground electric field induced by the same magnetic storm but recorded at MCQ, a high-latitude observatory. Figure 3 (right four panels) shows snapshots of the ground electric field at four times where the majority of sites have their peak magnitude.

To illustrate the differing contributions of high-latitude and mid-latitude magnetic-field variations, we calculate a ratio as  $E_{max\_MCQ} / E_{max\_CNB}$  at each site. When referenced to the CNB data, the increases in the peak electric field derived using MCQ data are shown across the majority of the study area, with peak electric field enhanced by a factor of 1.1 to 2.

## GEOMAGNETIC INDUCTION HAZARD

A colour-coded map in Figure 4 shows estimating the peak electric fields that occurred over the region during the 1989 storm as recorded at CNB. Over most of the Murray and Eromanga basins, which are distant from the ocean, the ground electric fields are relatively weak – less than 100 mV/km. In the Musgrave Province, Gawler Craton, Lachlan Fold Belt and New England Fold Belt, the ground electric fields are consistently strong – reaching 1000 to 2000 mV/km at most sites and even up to 5000 mV/km at several sites.



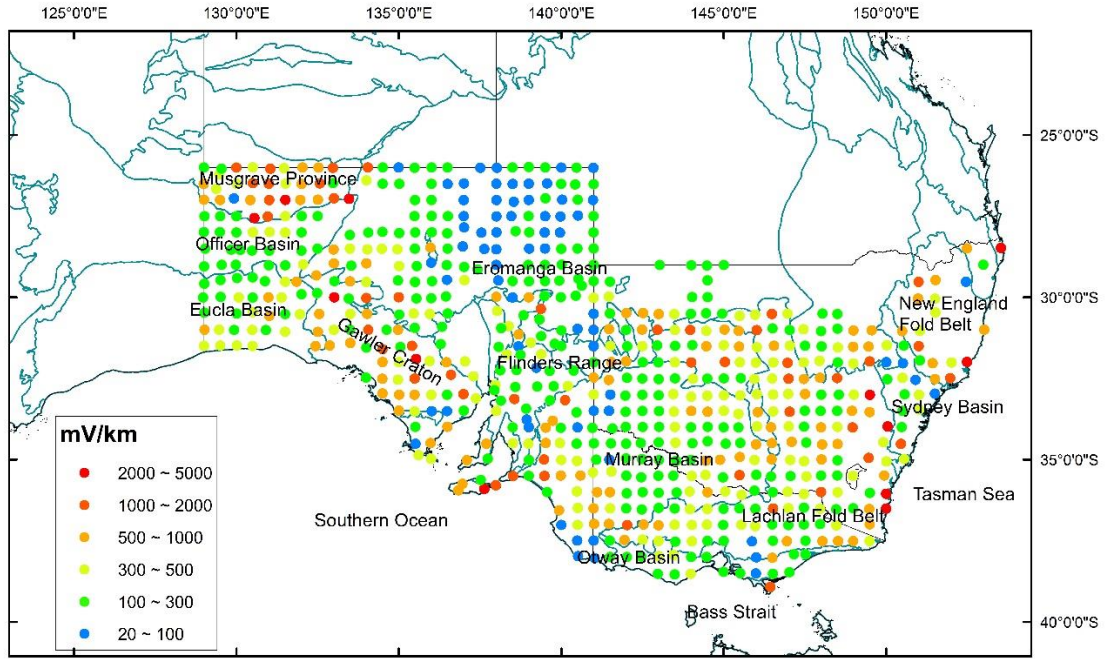


**Figure 4. Peak ground electric field during the 1989 Québec storm as recorded at Canberra geomagnetic observatory.**

The influence of proximal deeper oceans manifests as enhancement of ground electric fields in the Eucla Basin, typically in the range 300 to 500 mV/km. The Eucla Basin is adjacent to the Great Australian Bight where the coastline drops abruptly over a relatively narrow continental shelf into Southern Ocean waters up to 4 km deep. The Otway Basin in Victoria is adjacent to Bass Strait where water depths are typically 50-70 m. The Otway Basin conductivity anomaly (Lilley and Bennett, 1972) also contributes to weaker ground electric fields of <100 mV/km. The Tasman Sea adjacent to the Sydney Basin is much shallower than the Southern Ocean. The difference in typical ground electric fields in these areas can be explained by the difference in ocean depths adjacent to the Eucla, Otway and Sydney basins and is a manifestation of the well-known geomagnetic coast effect (e.g. Lilley, 2007) expressed in a 3D conductivity structure.

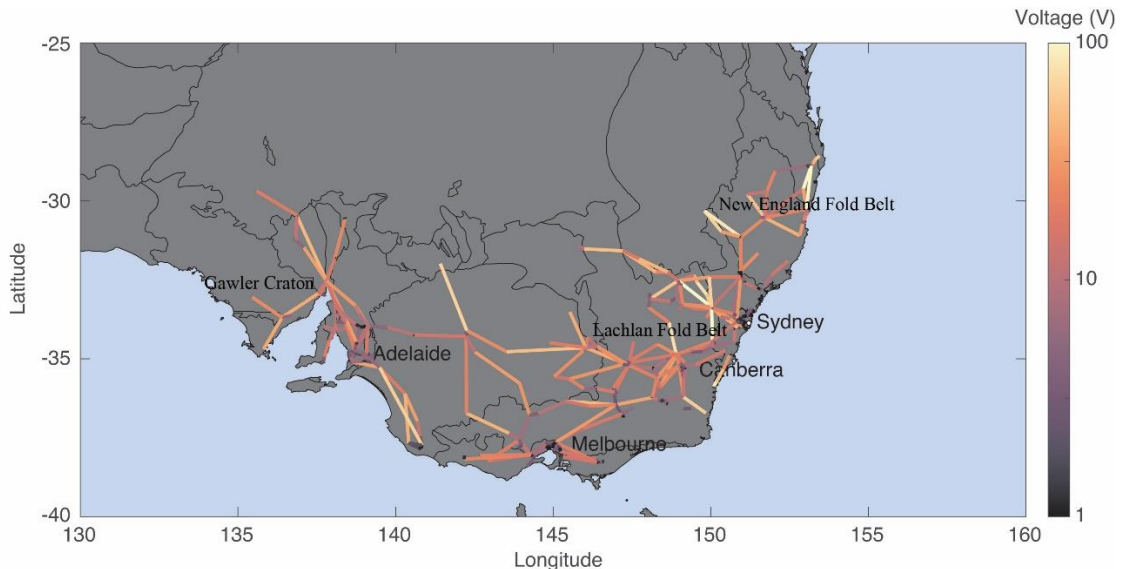


**Figure 5. Peak geomagnetically induced voltage during the 1989 Québec storm in the high-voltage grid.**

Figure 5 depicts the peak induced voltages in the Australian high voltage network which is a line integral of the geoelectric field (Figure 4) on the straight-line path from two connecting ground node substations during the scenario analysis of the 1989 Québec storm. It appears that transmission lines approximately perpendicular to the shoreline have a relative larger line voltage (bright yellow) than those that are approximately parallel to the shoreline. However the amplitude of line voltage depends on the dominant geoelectric field direction, the length of the transmission line path, and the network topology. Note that the two lines parallel to the shoreline near the top of the New England fold belt

region are primarily influenced by a single MT site (Figure 4), and their large line voltages are not realistically estimated.

## CONCLUSIONS

We modelled peak geoelectric field values induced by the 1989 Québec storm for south-eastern Australian states using a scenario analysis. The “geomagnetic hazard map” in Figure 4 shows the 3D subsurface geology has a great impact on GICs. In the Musgrave Province, Gawler Craton, Lachlan Fold Belt and New England Fold Belt, the ground electric fields are consistently strong compared to those in the conductive basins. We also compared the peak geoelectric field values by using the same magnetic storm event recorded at different latitudes, as reflected by the data from the CNB and MCQ geomagnetic observatories. In the presence of 3D geology, the peak geoelectric field is associated with not only the intensity of the inducing geomagnetic field variations, but also their polarisation orientation and frequency content.

We presented estimations of the geomagnetically induced voltage along transmission line paths by taking into account the magnitude and polarisation of the ground geoelectric field. Geomagnetically induced voltages in the Australian high-voltage power grid estimated using the scenario analysis could be in excess of 100 V in some transmission lines. Realistic peak geoelectric field could further be scaled up by 20 ~ 40% due to band-limited analysis.

## ACKNOWLEDGMENTS

This research is published with permission of the CEO, Geoscience Australia. The authors thank Geoscience Australia, the Geological Survey of Victoria, the Geological Survey of South Australia, the Geological Survey of New South Wales, the University of Adelaide and AuScope for making their MT datasets available for investigation.

## REFERENCES

- Cagniard, L., 1953, Basic theory of the magneto-telluric method of geophysical prospecting: *Geophysics*, 18(3), 605–635.
- Bartlett, S., 2016, Trans-Australian HVDC interconnection investigation, Paper presented at 2016 IEEE PES Asia-Pacific Power and Energy Engineering Conference, Xi'an, China. 10.1109/APPEEC.2016.7779587.
- Blais, G., and Metsa, P., 1993, Operating the Hydro-Québec grid under storm conditions since the storm of 13 March 1989. In J. Hruska, M. A. Shea, D. F. Smart, & G. Heckman (Eds.), *Proceedings of the Solar-Terrestrial Predictions Workshop*, Ottawa, May 18 22, 1992 (Vol. 1). Boulder, CO: NOAA.
- Boteler, D. H., 2019, A 21st century view of the March 1989 magnetic storm: *Space Weather*, 17, 1427–1441. <https://doi.org/10.1029/2019SW002278>.
- Duan, J., and Kyi, D., 2018, Australian Lithospheric Architecture Magnetotelluric Project (AusLAMP): Victoria Data Release Report (Technical Report), Canberra, ACT: Geoscience Australia. [pid.geoscience.gov.au/dataset/ga/120864](http://pid.geoscience.gov.au/dataset/ga/120864).
- Eastwood, J. P., Biffis, E., Hapgood, M. A., Green, L., Bisi, M. M., Bentley, R. D., Wicks, R., McKinnell, L. A., Gibbs, M., and Burnett, C., 2017, The economic impact of space weather: Where do we stand?: *Risk Analysis*, 37(2), 206–218. doi: 10.1111/risa.12765.
- Kyi, D., Duan, J., Kirkby, A. L. and Stolz, N., 2020, Australian Lithospheric Architecture Magnetotelluric Project (AusLAMP): New South Wales: data release (Phase one), Canberra, ACT: Geoscience Australia. <http://dx.doi.org/10.11636/Record.2020.011>
- Lilley, F. E. M., 2007, Coast effect of induced currents. In D. Gubbins & E. Herrero-Bervera (Eds.), *Encyclopedia of Geomagnetism and Paleomagnetism* (pp. 61–65). Dordrecht, Netherlands: Springer.
- Lilley, F. E. M., and Bennett, D. J., 1972, An array experiment with magnetic variometers near the coasts of south-east Australia: *Geophysical Journal of the Royal Astronomical Society*, 29, 49–64.
- Marshall, R. A., Wang, L., Paskos, G. A., Olivares-Pulido, G., van der Walt, T., et al., 2019, Modeling geomagnetically induced currents in Australian power networks using different conductivity models: *Space Weather*, 17(5), 727–756. <https://doi.org/10.1029/2018SW002047>.

Marshall, R. A., Dziura, L., Wang, L., Young, J., and Terkildsen, M., 2020, Estimating extreme geoelectric field values for the Australian region: *Space Weather*, 18, e2020SW002512. <https://doi.org/10.1029/2020SW002512>.

Orr, K., Allan, B., 2015, Electricity Transmission Lines. Geoscience Australia dataset. <http://pid.geoscience.gov.au/dataset/ga/83105>

Rastogi, R. G., 2006, Magnetic storm effects at equatorial electrojet stations: *Earth Planets and Space*, 58, 645–657.  
Robertson, K., Thiel, S., Gerrard, C., Gouthas, G., and Heath, P., 2018, MT data on SARIG: 2D and 3D resistivity models illuminate lithospheric scale structures and deep signatures of mineral systems. Retrieved from SARIG on 17 Feb 2020. [http://energymining.sa.gov.au/minerals/geoscience/geological\\_survey/gssa\\_projects/far\\_west/geophysics](http://energymining.sa.gov.au/minerals/geoscience/geological_survey/gssa_projects/far_west/geophysics).

Schrijver, C. J., Dobbins, R., Murtagh, W., and Petrinec, S. M., 2014, Assessing the impact of space weather on the electric power grid based on insurance claims for industrial electrical equipment: *Space Weather*, 12 (7), 487–498.

Schulte in den Bäumen, H., Moran, D., Lenzen, M., Cairns, I., and Steenge, A., 2014, How severe space weather can disrupt global supply chains: *Natural Hazards and Earth System Sciences*, 14(10), 2749–2759.

Wang, L., Hitchman, A. P., Ogawa, Y., Siripunvaraporn, W., Ichiki, M., and Fuji-ta, K., 2014, A 3-D conductivity model of the Australian continent using observatory and magnetometer array data: *Geophysical Journal International*, 198(2), 1171–1186. <https://doi.org/10.1093/gji/ggu188>.

Wang, L., Lewis, A. M., Ogawa, Y., Jones, W. V., and Costelloe, M. T., 2016, Modeling geomagnetic induction hazards using a 3-D electrical conductivity model of Australia: *Space Weather*, 14, 1125–1135. <https://doi.org/10.1002/2016SW001436>.

Wang, L., Duan, J., Hitchman, A. P., Lewis, A. M., and Jones, W. V., 2020, Modeling geoelectric fields induced by geomagnetic disturbances in 3D subsurface geology, an example from southeastern Australia: *Journal of Geophysical Research: Solid Earth*, 125, e2020JB019843. <https://doi.org/10.1029/2020JB019843>.